# Mutational tests of the NMR-docked structure of the staphylococcal nuclease-metal-3′,5′-pdTp complex

**ARTICLE** *in* PROTEINS STRUCTURE FUNCTION AND BIOINFORMATICS · SEPTEMBER 1993

Impact Factor: 2.63 · DOI: 10.1002/prot.340170107 · Source: PubMed



**4 AUTHORS**, INCLUDING:

Woei-Jer Chuang
National Cheng Kung University
**91** PUBLICATIONS **1,298** CITATIONS
SEE PROFILE

David Joseph Weber
University of Maryland, Baltimore
**126** PUBLICATIONS **3,822** CITATIONS
SEE PROFILE

Apostolos G Gittis
National Institute of Allergy and Infectious …
**42** PUBLICATIONS **2,093** CITATIONS
SEE PROFILE

PROTEINS: Structure, Function, and Genetics 17:36–48 (1993)

# Mutational Tests of the NMR-Docked Structure of the Staphylococcal Nuclease–Metal–3′,5′-pdTp Complex

**Woei-Jer Chuang,[1] David J. Weber,[1] Apostolos G. Gittis,[2] and Albert S. Mildvan[1]**

*Departments of [1]Biological Chemistry and [2]Biophysics and Biophysical Chemistry, The Johns Hopkins University School of Medicine, Baltimore, Maryland 21205*

***ABSTRACT*** **In the X-ray structure of the staphylococcal nuclease–$Ca^{2+}$–3′,5′-pdTp complex, the conformation of the inhibitor 3′,5′-pdTp is distorted by Lys-70* and Lys-71* from an adjacent molecule of staphylococcal nuclease (Loll, P.J., Lattman, E.E. Proteins 5:183–201, 1989). In order to correct this crystal packing problem, the solution conformation of enzyme-bound 3′,5′-pdTp in the staphylococcal nuclease–metal–pdTp complex determined by NMR methods was docked into the X-ray structure of the enzyme [Weber, D.J., Serpersu, E.H., Gittis, A.G., Lattman, E.E., Mildvan, A.S. (preceding paper)]. In the NMR-docked structure, the 5′-phosphate of 3′,5′-pdTp overlaps with that in the X-ray structure. However the 3′-phosphate accepts a hydrogen bond from Lys-49 (2.89 Å) rather than from Lys-84 (8.63 Å), and N3 of thymine donates a hydrogen bond to the OH of Tyr-115 (3.16 Å) which does not occur in the X-ray structure (5.28 Å). These interactions have been tested by binding studies of 3′,5′-pdTp, $Ca^{2+}$, and $Mn^{2+}$ to the K49A, K84A, and Y115A mutants of staphylococcal nuclease using water proton relaxation rate and EPR methods. Each mutant was fully active and structurally intact, as found by CD and two-dimensional NMR spectroscopy, but bound $Ca^{2+}$ 9.1- to 9.9-fold more weakly than the wild-type enzyme. While the K84A mutation did not significantly weaken 3′,5′-pdTp binding to the enzyme (1.5 ± 0.7 fold), the K49A mutation weakened 3′,5′-pdTp binding to the enzyme by the factor of 4.4 ± 1.8-fold. Similarly, the Y115A mutation weakened 3′,5′-pdTp binding to the enzyme 3.6 ± 1.6-fold. Comparable weakening effects of these mutations were found on the binding of $Ca^{2+}$–3′,5′-pdTp. These results are more readily explained by the NMR-docked structure of staphylococcal nuclease–metal–3′,5′-pdTp than by the X-ray structure.**



**Key words: staphylococcal nuclease, mutants of, lattice artifacts, dissociation constants of 3′,5′-pdTp, subdomains of, $Ca^{2+}$ binding to**



## INTRODUCTION

Staphylococcal nuclease (EC 3.1.4.7) is a $Ca^{2+}$-activated enzyme which catalyzes the hydrolysis of phosphodiester linkages in both DNA and RNA to yield 3′-mononucleotides, oligonucleotides, and polynucleotides. The structure of the ternary complex of the enzyme, $Ca^{2+}$, and the competitive inhibitor 3′,5′-pdTp* has been studied by X-ray diffraction[1,2] and NMR spectroscopy.[3–6] In the X-ray structure of the enzyme–$Ca^{2+}$–3′,5′-pdTp complex (Fig. 1A), the conformation of 3′,5′-pdTp is distorted by Lys-70* and Lys-71* from an adjacent enzyme molecule in the crystal lattice.[2,7] The thymine of 3′,5′–pdTp makes no specific contacts with the nuclease and its N3 and O4 are hydrogen bonded to a string of water molecules occupying the top of the active site. The 3′-phosphate is hydrogen bonded to the side chains of Lys-84 and Tyr-85, the 5′-phosphate is coordinated to $Ca^{2+}$, and its oxygens are involved in hydrogen bonding with Arg-35 and Arg-87 (Fig. 1A).

To eliminate the lattice artifact, the undistorted conformation of enzyme bound 3′,5′-pdTp in the staphylococcal nuclease–metal–pdTp complex was determined in solution. This undistorted conformation of the enzyme-bound metal-inhibitor complex was docked into the X-ray structure of staphylococcal nuclease by superimposing the metals and by using 19 intermolecular NOEs from ring protons of Tyr-85, Tyr-113, and Tyr-115 to protons of 3′,5′-pdTp (Fig. 1B).[6] While the 5′-phosphate of the NMR-docked pdTp overlaps with that in the X-ray structure, the positions of the 3′-phosphate, deoxyribose,

*Abbreviations used: 3′,5′-pdTp, thymidine 3′,5′-diphosphate; Tris-DCl, tris(hydroxymethyl)aminomethane-deuterium chloride; NOESY, nuclear Overhauser effect spectroscopy; CD, circular dichroism; Lys-70*, 71*, lysine residues from a neighboring molecule of staphylococcal nuclease in the crystal lattice.

Received February 8, 1993; revision accepted April 20, 1993.

Address reprint requests to Dr. Albert S. Mildvan, Department of Biological Chemistry, The Johns Hopkins University School of Medicine, 725 North Wolfe Street, Baltimore, MD 21205-2185.

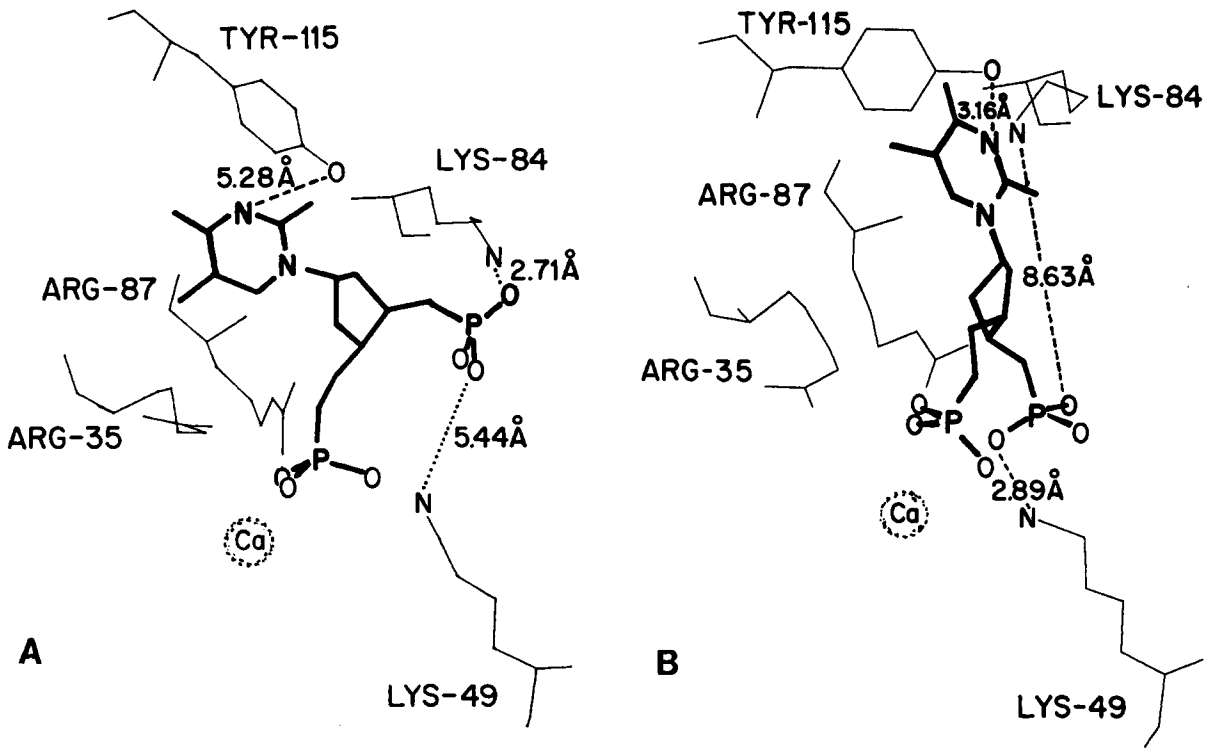


Fig. 1. Schematic diagram of the active site of staphylococcal nuclease in X-ray (**A**) and NMR-docked structure (**B**) illustrating the hydrogen-bonding interactions between residues K49, K84, and Y115 of staphylococcal nuclease and 3′,5′-pdTp.

**TABLE I. Distances (Å) Between Residues of Staphylococcal Nuclease and 3′,5′-pdTp***

| | | Thymine | | 3′-Phosphate | | |
|---|---|---|---|---|---|---|
| Residue | Method | N3 | O2 | O1 | O2 | O3 |
| K49 (Nϵ) | NMR† | 11.35 | 9.64 | 2.89 | 3.02 | 4.15 |
| | X-ray‡ | 12.42 | 12.12 | 8.72 | 7.81 | 7.76 |
| K84 (Nϵ) | NMR† | 3.53 | 4.74 | 9.73 | 9.78 | 8.63 |
| | X-ray‡ | 7.96 | 5.89 | 2.71 | 3.70 | 6.91 |
| Y85 (Oζ) | NMR† | 6.09 | 5.13 | 6.85 | 6.24 | 4.85 |
| | X-ray‡ | 9.59 | 7.74 | 3.89 | 2.69 | 5.06 |
| Y115 (Oζ) | NMR† | 3.16 | 4.32 | 11.32 | 10.97 | 11.19 |
| | X-ray‡ | 5.28 | 5.07 | 7.25 | 8.42 | 6.99 |

*Distances ≤3.5 Å are assumed to be hydrogen bonded.
†From Weber et al.[6]
‡From Loll and Lattman.[2]

and thymine rings differ significantly from those found in the X-ray structure (Fig. 1). Thus, in the NMR-docked structure the 3′-phosphate of pdTp accepts a H-bond from Lys-49 (2.89 Å) rather than from Lys-84 (8.63 Å) or from Tyr-85 (4.85 Å), and the N3 of thymine donates a H-bond to the OH of Tyr-115 (3.16 Å) which does not occur in the X-ray structure (5.28 Å). Table I compares distances from Lys-49, Lys-84, Tyr-85, and Tyr-115 of staphylococcal nuclease to the thymine and 3′-phosphate of bound 3′,5′-pdTp in the X-ray and NMR-docked structures.

In accord with the NMR-docked structure, a kinetic analysis of the Y85F mutant of staphylococcal nuclease[8] detected no significant effects on the $K_M$ values of substrates with either a 3′-phosphate or a 3′-phosphonate, but revealed a 14-fold decrease in $k_{cat}$ with the former substrate, suggesting an interaction between the 3′-phosphate and Tyr-85 at a later stage of the reaction, subsequent to binding.

As a further test of the NMR-docked versus the X-ray structure of the ternary staphylococcal nuclease–$Ca^{2+}$–3′,5′-pdTp complex, we have studied the binding of 3′,5′-pdTp, $Mn^{2+}$, and $Ca^{2+}$ to the fully active K49A, K84A, and Y115A mutants of the

**TABLE II. Kinetic Parameters of Wild-Type, K49A, K84A, and Y115A Mutants of Staphylococcal Nuclease***

| Enzyme | $K_M^{Ca}$ (μM) | $K_M^{DNA}$ (μg/ml) | $K_A^{Ca}$ (μM) | $K_S^{DNA}$ (μg/ml) | Relative $V_{max}$ |
|---|---|---|---|---|---|
| WT | 110 ± 20 | 3.5 ± 0.8 | 460 ± 60 | 17.9 ± 0.7 | 1.00 ± 0.06 |
| K49A | 617 ± 111 | 6.31 ± 0.53 | 2125 ± 256 | 12.26 ± 3.60 | 0.96 ± 0.06 |
| K84A | 1318 ± 66 | 6.91 ± 1.24 | 3189 ± 383 | 11.29 ± 0.36 | 1.08 ± 0.09 |
| Y115A | 881 ± 132 | 7.18 ± 0.6 | 2714 ± 271 | 24.28 ± 4.37 | 1.82 ± 0.17 |

*$K_M^{Ca}$ is the Michaelis constant of $Ca^{2+}$ at saturating [DNA], $K_M^{DNA}$ is the Michaelis constant of [DNA] at saturating $Ca^{2+}$, $K_A^{Ca}$ is the $K_M$ of $Ca^{2+}$ extrapolated to zero [DNA], and $K_S^{DNA}$ is the $K_M$ of DNA extrapolated to zero [$Ca^{2+}$]. The parameters for the wild-type enzyme are from Serpersu et al.[12] $V_{max}$ of wild type is 0.714 ± 0.04 Δ Abs $min^{-1}$ $mg^{-1}$.

enzyme by EPR and by the longitudinal relaxation rate of water protons. Lowered affinities of the K49A and Y115A mutants for 3′,5′-pdTp are found, consistent with the NMR docked structure.

## MATERIALS AND METHODS

### Materials

The nucleotide 3′,5′-pdTp was obtained from P-L Biochemicals (Division of Pharmacia), and its concentration was determined using the extinction coefficient at 260 nm of 9600 $M^{-1}$ $cm^{-1}$. Before use, buffer and nucleotide solutions were passed over Chelex 100 resin to remove trace metals. Salmon sperm DNA was purchased from Sigma, and all DNA used in the enzyme assay was denatured by boiling for 30 min followed by rapid cooling on ice and passage over Chelex 100 resin.[9]

### Methods

#### *Isolation of enzymes*

The preparation, DNA isolation, and sequence analysis of all mutations in the staphylococcal nuclease gene were done as previously described.[10] The purification of all mutant enzymes was performed as described previously for the purification of the wild-type enzyme.[11]

#### *Enzyme assay*

The enzyme activity was monitored by observing the absorbance increase at 260 nm as DNA is hydrolyzed.[9] One unit of enzymatic activity is defined as the amount of enzyme causing a change of 1.0 absorbance unit per minute at 260 nm in a 1-cm cell. Protein concentrations of the wild-type, K49A, and K84A mutant enzymes were determined by the absorbance at 280 nm ($\epsilon^{0.1\%} = 0.93$) at pH 7.4. For the Y115A mutant, the extinction coefficient of 0.84 was determined by Bradford protein assay (Bio-Rad Protein Assay) with wild-type nuclease as standard.

#### *Analysis of kinetic data*

The data obtained from enzyme assays were plotted in double-reciprocal form as initial velocity vs the concentration of free $Ca^{2+}$, and as initial velocity vs the concentration of DNA as previously described.[12,13] For each mutant, initial reaction rates were measured at 5 concentrations of $Ca^{2+}$ ranging from 1.0 to 25.0 mM and at 5 concentrations of DNA ranging from 10 to 60 μg/ml. Secondary plots were made from extrapolations of these primary plots to obtain $K_A^{Ca}$, $K_M^{DNA}$, $K_S^{DNA}$, $K_M^{Ca}$, and $V_{max}$. In the analyses of all of the kinetic data, lines in the primary plots were computed by a weighted least-squares analysis,[14] and the lines in the secondary plots were computed by an unweighted least-squares analysis.

#### *CD spectroscopy*

CD spectra were measured at 27°C on an AVIV 60DS spectropolarimeter that was calibrated with camphosulfonic acid.[15] Spectra were recorded between 185 and 260 nm using a 0.1-mm quartz cell. The samples contained 1.0 mg/ml wild-type or mutant enzymes and 40 mM Tris-HCl, pH 7.4, in the absence or presence of 5 mM 3′,5′-pdTp and 31 mM $CaCl_2$. A 1.0-nm spectral step size, a 1.0-nm bandwidth, and a 12 nm/min scan rate were employed. The final spectra obtained were the average of five scans and were corrected by five scans of the solvent alone. The ellipticity is reported as the mean residue ellipticity, θ in units of deg $cm^2$/dmol. The secondary structure of the enzymes were estimated by using the convex constraint algorithm (CCA) together with a least-square-fitting program (LINCOMB) as described by Perczel et al.[16,17] Attempts to fit the CD data were also made using the basis set of Yang et al.[18]

#### *$^1H$ NMR spectroscopy*

All proton NMR spectra were obtained at 600 MHz with a Bruker AM 600 NMR spectrometer. Samples with the enzyme alone (1.8 mM) contained 30 mM NaCl and 10 mM ($d_{11}$) Tris-DCl, in a total volume of 0.5 ml. Samples with $Ca^{2+}$ and 3′,5′-pdTp contained 1.7 mM $CaCl_2$ and 9.4 mM ($d_{11}$) Tris-DCl, in a volume of 0.53 ml. The pH of each sample was measured to be 7.4 in $H_2O$. Each sample was then lyophilized twice and redissolved in $^2H_2O$. NOESY

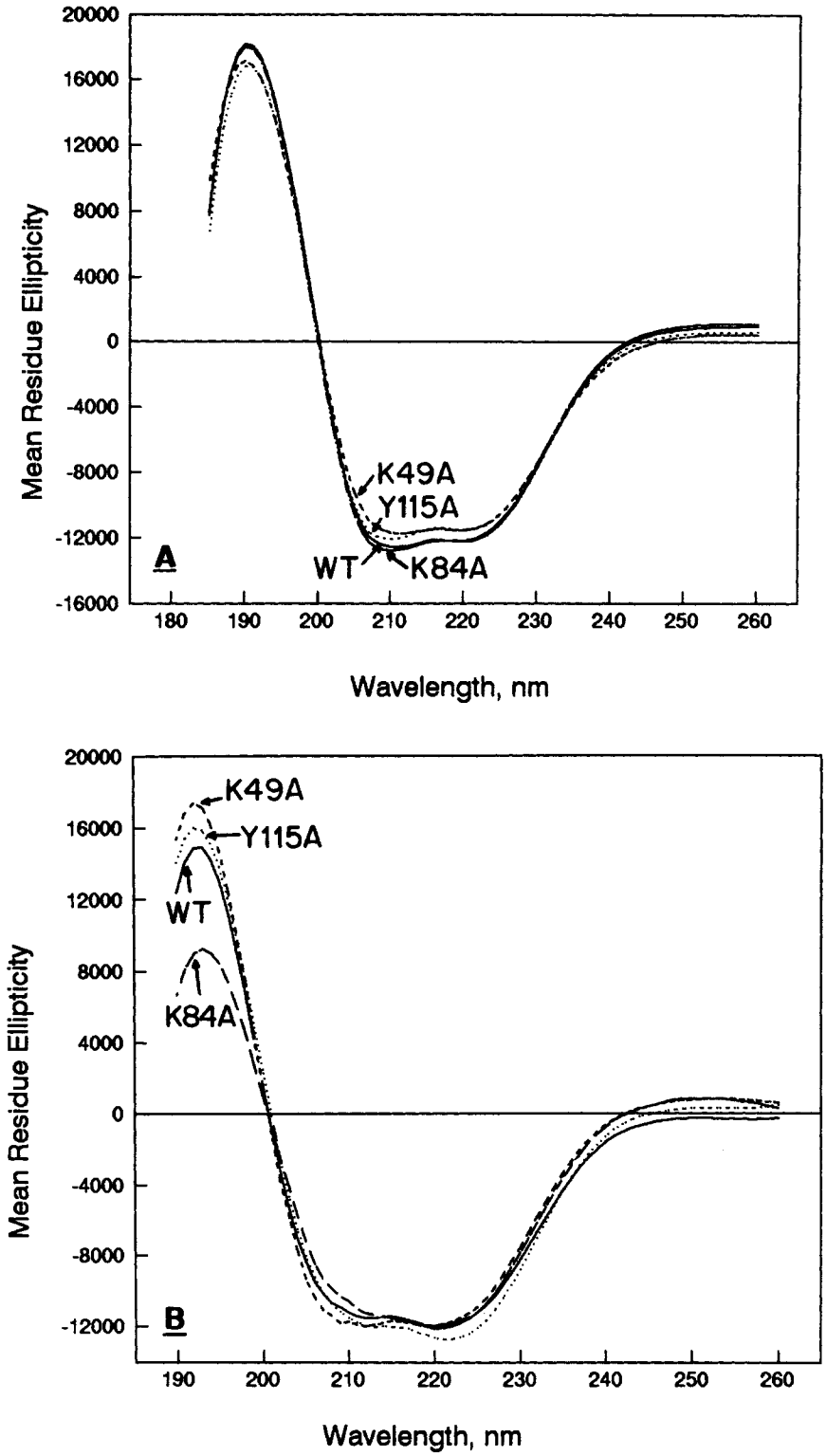


Fig. 2. Circular dichroism spectra of wild-type (——) and K49A (- - -), K84A (– – –), and Y115A (· · ·) staphylococcal nuclease in the absence (**A**) or presence (**B**) of 5 mM $Ca^{2+}$ and 31 mM 3′,5′-pdTp.

spectra[19] were acquired in the phase-sensitive mode by using time-proportional phase incrementation (TPPI)[20] with a 100-msec mixing time. The parameters for acquisition of NOESY spectra included a 1.15 sec relaxation delay, a 0.145 sec acquisition time, a 7042 Hz sweep width, 2K data points in F2

**TABLE III. Secondary Structures of Wild-Type and Mutant Staphylococcal Nuclease as Determined by CD, and Comparison With X-Ray and NMR Studies**

| | | Staph nuclease* | | | Staph nuclease-$Ca^{2+}$-3′,5′-pdTp† | | |
|---|---|---|---|---|---|---|---|
| Enzyme | Method | α-Helix (%) | β-Structure (%) | Coil (%) | α-Helix (%) | β-Structure (%) | Coil (%) |
| WT | X-ray‡,§ | 24.2 | 41.6 | 34.2 | 24.2 | 39.6 | 36.2 |
| WT | NMR**,†† | 24.2 | 38.2 | 37.6 | 27.5 | 38.3 | 34.2 |
| WT | CD | 25 | 38.4 | 36.6 | 27.5 | 37.9 | 34.6 |
| K49A | CD | 26.7 | 33.8 | 39.5 | 24.5 | 43.7 | 31.8 |
| K84A | CD | 24.3 | 38.5 | 37.2 | 29.1 | 32.3 | 38.6 |
| Y115A | CD | 26 | 34.5 | 39.6 | 29.9 | 35.4 | 34.7 |

*The root mean square deviations of the fit in WT, K49A, K84A, and Y115A are 3.4, 5.4, 4.8, and 5.1%, respectively.
†The root mean square deviations of the fit in WT, K49A, K84A, and Y115A are 4.5, 5.7, 5.3, and 5.5%, respectively.
‡Free staphylococcal nuclease.[26]
§Ternary complex.[2]
**Free enzyme.[27]
††Ternary complex.[4]

and 768 data points in F1, and a filter width of 22 kHz. The data were processed on a personal IRIS (Silicon Graphics Inc.) using the software Felix (Hare Research Inc.). The time domain data sets were zero-filled in F1 to 2K and were multiplied by a squared sine-bell function shifted by 30° prior to the Fourier transformation.

### *Metal and 3′,5′-pdTp binding studies*

The binding of $Mn^{2+}$ and 3′,5′-pdTp to all mutants was monitored by changes in the paramagnetic effects of $Mn^{2+}$ on the longitudinal ($1/T_1$) relaxation rate of water protons, measured with a Seimco pulsed NMR spectrometer at 24.3 MHz with a 180°-τ-90° pulse sequence as previously described.[12,21,22] The observed enhancement of relaxation rate is defined as $\epsilon^* = (1/T_{1p}^*)/(1/T_{1p})$, where $(1/T_{1p})$ is the paramagnetic contribution to the longitudinal relaxation rate in the presence (*) and absence of enzyme.[22]

In $Mn^{2+}$-binding studies, the concentration of free $Mn^{2+}$ in a mixture of free and bound $Mn^{2+}$ was determined by electron paramagnetic resonance[23] with a Varian E-4 EPR spectrometer. The NMR and EPR data were analyzed as previously described[12,13,22,24] to determine the stoichiometry ($n$) of $Mn^{2+}$ bound to each mutant, the dissociation constant ($K_D$), and the enhancement factor ($\epsilon_b$) of the binary enzyme–$Mn^{2+}$ complex. The binding of $Mn^{2+}$ to the enzyme-3′,5′-pdTp complex was also monitored both by EPR and by changes in $1/T_{1p}^*$ of water protons, providing an independent measurement of the dissociation constant ($K_A'$) of $Mn^{2+}$ from ternary complexes. Titrations of the binary enzyme–$Mn^{2+}$ complexes with 3′,5′-pdTp monitoring changes in $1/T_{1p}$ of water protons were carried out and analyzed by computer as previously described[13,22,25] to give dissociation constants ($K_2$,$K_3$) and enhancement factors ($\epsilon_T$) of ternary complexes. The dissociation constants for binary and ternary $Ca^{2+}$ complexes were obtained by competition experiments in which the corresponding $Mn^{2+}$ complex was titrated with $Ca^{2+}$, monitoring the displacement of $Mn^{2+}$ by the decrease in the enhancement ($\epsilon^*$) of $1/T_{1p}$ of water protons, and independently by the appearance of free $Mn^{2+}$ in the EPR spectrum, as previously described.[12,13] The dissociation constants $K_D$ and $K_A'$ for $Ca^{2+}$ were calculated from the relationship $K^{Ca} = K_{App}^{Ca}/(1 + [Mn^{2+}]/K^{Mn})$ where $K_{App}^{Ca}$ is the apparent $K_D$ or $K_A'$ for $Ca^{2+}$ used to fit the $Mn^{2+}$ displacement titration curve, and $K^{Mn}$ is the directly measured $K_D$ or $K_A'$ for $Mn^{2+}$.

## RESULTS

### Kinetic Studies of the K49A, K84A, and Y115A Mutants of Staphylococcal Nuclease

Detailed kinetic analyses of the activation by $Ca^{2+}$ at varying levels of DNA were carried out for the K49A, K84A, and Y115A mutants, as previously described for the wild-type enzyme.[12] Table II summarizes the kinetic parameters obtained from these data and compares them with those of the wild-type enzyme obtained under identical conditions.[12] From the $V_{max}$ values it is clear that all of the mutants are fully active, indicating that Lys-49, Lys-84 and Tyr-115 are not directly involved in catalysis. The Y115A mutant shows a 1.8-fold greater $V_{max}$ than the wild type and a 2.05-fold greater $K_M^{DNA}$. The K49A and K84A mutants show similar $V_{max}$ values to that of wild type but a 2-fold greater $K_M^{DNA}$. Hence all of the mutations have small weakening effects on DNA binding in the active ternary com-

Fig. 3. 2D $^1H$ NOESY spectra in $^2H_2O$ of wild-type (black) and K49A (blue), K84A (red), and Y115A (purple) mutants of staphylococcal nuclease. The upfield region (**A**) and the downfield aromatic region (**B**) are shown. The mixing time was 100 msec. Other parameters are given in Methods.

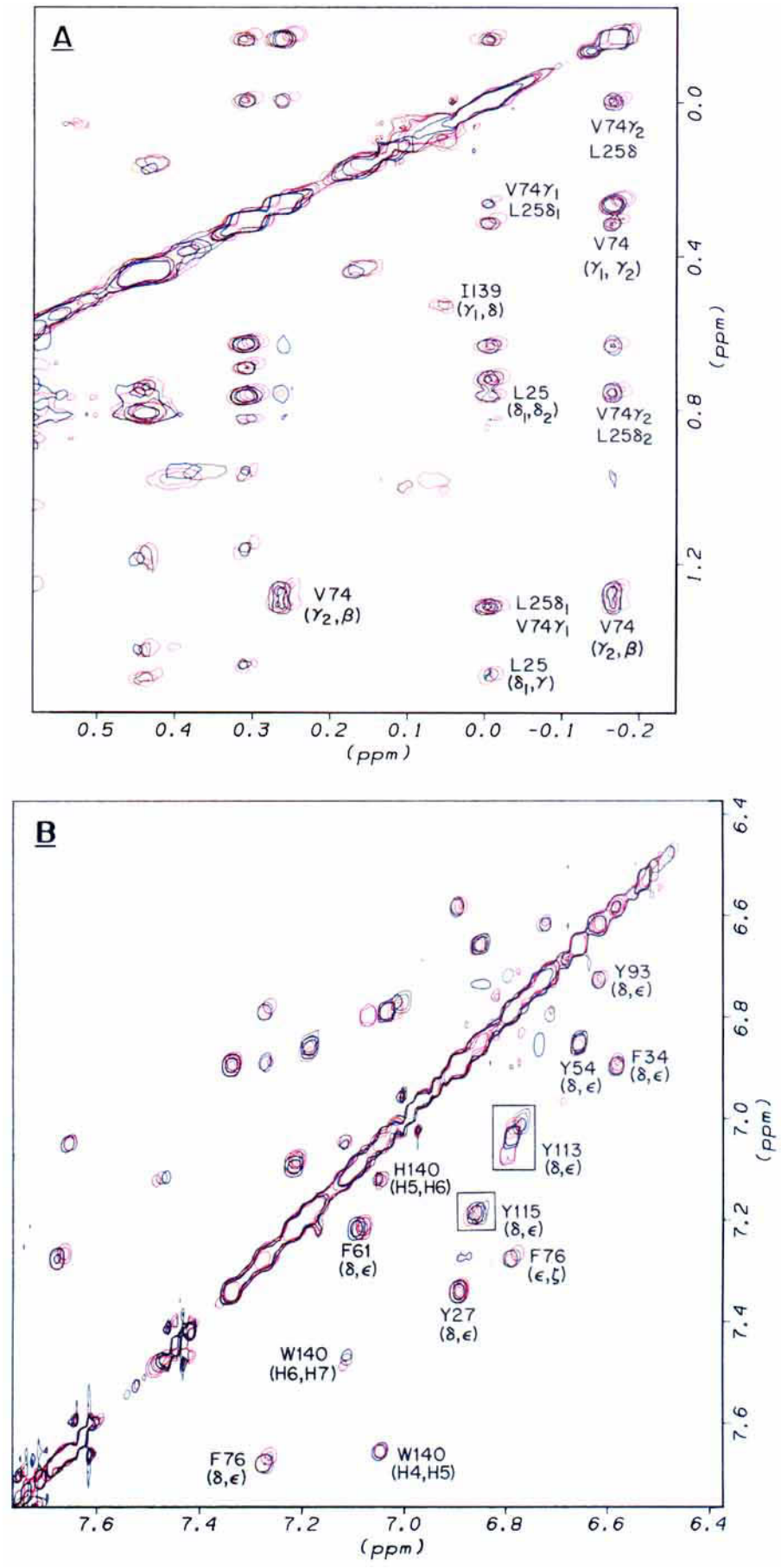
A
V74γ2
L25δ
V74γ1
L25δ1
V74
(γ1, γ2)
I139
(γ1, δ)
L25
(δ1, δ2)
V74γ2
L25δ2
V74
(γ2, β)
L25δ1
V74γ1
V74
(γ2, β)
L25
(δ1, γ)
0.0
0.4
0.8
1.2
(ppm)
0.5 0.4 0.3 0.2 0.1 0.0 -0.1 -0.2
(ppm)
B
Y93
(δ, ε)
Y54
(δ, ε)
F34
(δ, ε)
Y113
(δ, ε)
H140
(H5, H6)
Y115
(δ, ε)
F61
(δ, ε)
F76
(ε, ζ)
Y27
(δ, ε)
W140
(H6, H7)
F76
(δ, ε)
W140
(H4, H5)
6.4
6.6
6.8
7.0
7.2
7.4
7.6
(ppm)
7.6 7.4 7.2 7.0 6.8 6.6 6.4
(ppm)

Fig. 3.

plexes as reflected in $K_M^{DNA}$. All three mutations significantly weaken $Ca^{2+}$ binding to the free enzyme as detected by 4.6- to 6.9-fold increases in $K_A^{Ca}$, and to the enzyme–DNA complex as detected by 5.6- to 12-fold increases in $K_M^{Ca}$. As previously found with mutants of Arg-35 and Arg-87, $Ca^{2+}$ binding is unusually sensitive to mutations of residues which are not directly coordinated by the metal.[13]

### Structural Studies of Wild-Type and Mutants of Staphylococcal Nuclease by CD Spectroscopy

CD spectroscopy was used to compare secondary structures of wild-type and mutant enzymes in the absence and presence of 5 mM 3′,5′-pdTp and 31 mM $CaCl_2$. The CD spectra of the wild-type, K49A, K84A, and Y115A mutant enzymes are all very similar (Fig. 2A), and were fit with a root mean square deviation (RMSD) of 3.4–5.7% using the programs of Perczel et al.[16,17] The helix contents of the wild-type, K49A, K84A, and Y115A mutant enzymes were estimated to be 25, 26.7, 24.3, and 26%, respectively (Table III), values which are indistinguishable from that of the wild-type enzyme as found both by X-ray and NMR as 24.2%.[26,27] The other elements of secondary structure of the mutants agree within experimental error with those of the wild-type enzyme (Table III). An alternative fit of the CD spectra of the free enzyme with the basis set of Yang et al.[18] yielded slightly higher helix contents of 28.6, 29.7, 27.9, and 29.3% for the wild type, K49A, K84A, and Y115A enzymes, respectively, but were otherwise similar. For this reason we have used the procedure of Perczel et al.[16,17] in Table III. The addition of $Ca^{2+}$ and 3′,5′-pdTp slightly altered the CD spectra inducing some differences from that of the wild-type enzyme especially near 193 nm (Fig. 2B). Analysis of the CD data (Table III) revealed only small differences in secondary structure, considering the 4.5 to 5.7% errors in the fitting procedure, and reasonable agreement with the X-ray and NMR structures of the ternary complex of the wild-type enzyme.

### Structural Studies of Wild-Type and Mutants of Staphylococcal Nuclease by Two-Dimensional $^1H$ NMR Spectroscopy

$^1H$ NMR spectroscopy was also used to determine whether conformational differences exist between the wild-type, K49A, K84A, and Y115A mutant enzymes in the absence and presence of $Ca^{2+}$ and 3′,5′-pdTp. Most of the $^1H$, $^{15}N$, and $^{13}C$ chemical shift assignments have been determined for the ternary complex of the wild-type enzyme[3] and the H124L mutant staphylococcal nuclease in the absence and presence of $Ca^{2+}$ and 3′,5′-pdTp.[4,27] Our $^1H$ NOESY spectra, both in the absence and presence of $Ca^{2+}$ and 3′,5′-pdTp, indicate all of the mutant enzymes to be highly structured, and very similar to the wild-type enzyme. Minimal conformational differences between the mutant and wild-type free enzymes were reflected in negligible changes in chemical shifts for the upfield-shifted methyl protons (≤ 0.02 ppm, Fig. 3A) and for the aromatic protons (≤ 0.04 ppm, Fig. 3B). The cross peak between the δ and ϵ protons of Tyr-115 disappears in the Y115A mutant as expected. Similarly, in the presence of $Ca^{2+}$ and 3′,5′-pdTp the K49A, K84A, and Y115A mutants of staphylococcal nuclease showed minimal changes from the wild-type enzyme in the chemical shifts of the upfield methyl resonances (≤ 0.02 ppm, Fig. 4A) and in the chemical shifts of the aromatic resonances (≤ 0.04 ppm, Fig. 4B). A slightly larger shift of −0.12 ppm is found for the Y113δ resonance in the Y115A mutant, likely due to the loss of the ring current shielding effect of Tyr-115, and a shift of 0.06 ppm is found for the Y115ϵ resonance in the K84A mutant (Fig. 4B).

### Binary $Mn^{2+}$ and $Ca^{2+}$ Complexes of the K49A, K84A, and Y115A Mutants

The binding of $Mn^{2+}$ to all mutants was determined by two independent methods, EPR, which measures residual free $Mn^{2+}$, and the enhanced paramagnetic effects of bound $Mn^{2+}$ on the $1/T_1$ of water protons, which measures bound $Mn^{2+}$. The Scatchard plots based on the EPR data with the K49A, K84A, and Y115A mutants are shown in Figure 5A, and the dissociation constants ($K_D$) are given in Table IV. Like the wild-type enzyme, the mutants bind $Mn^{2+}$ at a single site but with dissociation constants which are 2.2- to 4.4-fold weaker. The enhancement factors of bound $Mn^{2+}$ ($\epsilon_b$) found with the mutants are greater than that of the wild-type enzyme, reflecting a different liganding environment of $Mn^{2+}$.

The competitive displacement of $Mn^{2+}$ by $Ca^{2+}$ from the binary complex of the mutants was monitored by both EPR and $1/T_1$ measurements. Titrations of the K49A, K84A, and Y115A mutants with $Ca^{2+}$ (Fig. 6), yielded dissociation constants ($K_D$(Ca)) for the binary enzyme–$Ca^{2+}$ complexes of 4.6 to 5.0 mM (Table V), which agree within a factor of 2 with $K_A^{Ca}$, the kinetically determined activator constants of $Ca^{2+}$ (Table II), and are 9.1- to 9.9-fold greater than the $K_D$(Ca) measured with the wild-type enzyme. Such order of magnitude weakening of $Ca^{2+}$ binding by the K49A, K84A, and Y115A mutations and the previously studied R35G and R87G mutations[13] are comparable to the effects of mutat-

Fig. 4. 2D $^1H$ NOESY spectra in $^2H_2O$ of wild-type (black) and K49A (blue), K84A (red), and Y115A (purple) mutants of staphylococcal nuclease in the presence of $Ca^{2+}$ and 3′,5′-pdTp. The upfield region (**A**) and the downfield aromatic region (**B**) are shown.

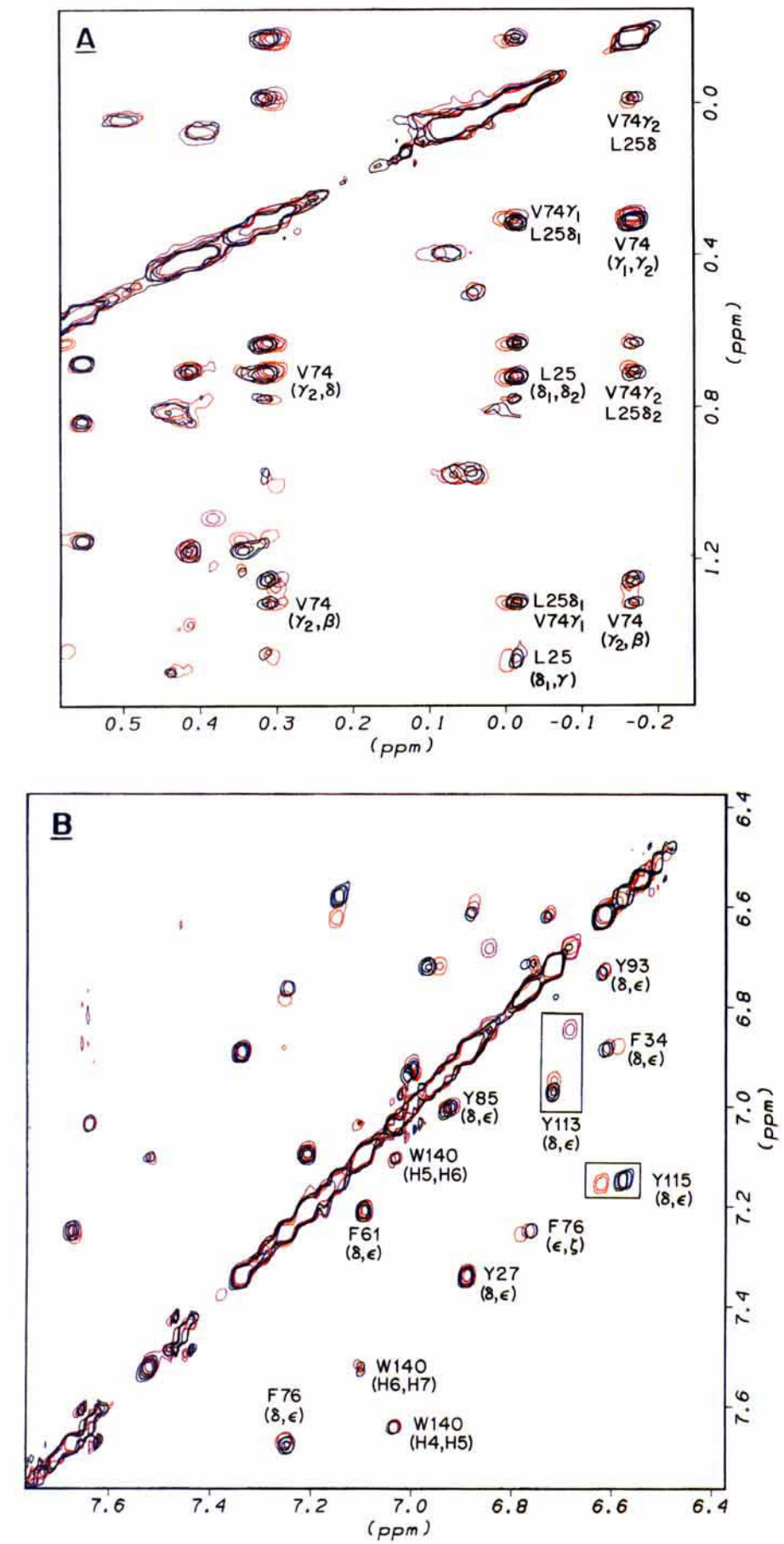
A
V74γ2
L25δ
V74γ1
L25δ1
V74
(γ1,γ2)
V74
(γ2,δ)
L25
(δ1,δ2)
V74γ2
L25δ2
V74
(γ2,β)
L25δ1
V74γ1
V74
(γ2,β)
L25
(δ1,γ)
0.0
0.4
0.8
1.2
(ppm)
0.5
0.4
0.3
0.2
0.1
0.0
-0.1
-0.2
(ppm)
B
Y93
(δ,ε)
F34
(δ,ε)
Y85
(δ,ε)
Y113
(δ,ε)
W140
(H5,H6)
Y115
(δ,ε)
F61
(δ,ε)
F76
(ε,ζ)
Y27
(δ,ε)
W140
(H6,H7)
F76
(δ,ε)
W140
(H4,H5)
6.4
6.6
6.8
7.0
7.2
7.4
7.6
(ppm)
7.6
7.4
7.2
7.0
6.8
6.6
6.4
(ppm)

Fig. 4.

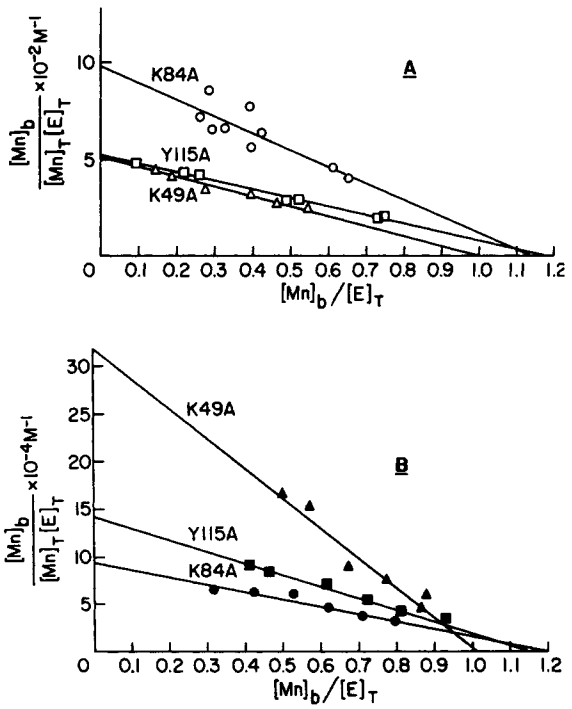


Fig. 5. Scatchard plots of binary and ternary complexes of mutant staphylococcal nuclease in the absence or presence of 3′,5′-pdTp with $Mn^{2+}$. (**A**) Titration of K49A (△), K84A (○), and Y115A (□) mutants of staphylococcal nuclease with $Mn^{2+}$. The concentrations of K49A, K84A, and Y115A are 483.3, 505.5, and 494.5 μM, respectively. (**B**) Titration of K49A (▲), K84A (●), and Y115A (■) mutants of staphylococcal nuclease and 3′,5′-pdTp with $Mn^{2+}$. The solutions contained 161.1 μM K49A with 163.7 μM pdTp, 253 μM K84A with 263 μM pdTp, and 164.5 μM Y115A with 175.3 μM pdTp. All solutions contained 40 mM Tris-HCl, pH 7.4, $T$ = 23°C.

ing Asp-21 and Asp-40 which are directly coordinated to $Ca^{2+}$.[12,13] Thus mutations of nonliganding residues at or near the active site produce structural differences in the immediate environment of the bound metal.

### Ternary Enzyme–$Mn^{2+}$–3′,5′-pdTp Complexes

The thermodynamics of a ternary system of enzyme, metal, and nucleotide is described by six interrelated equilibrium constants, which are defined in Table IV. $K_A'$(Mn), the dissociation constant of $Mn^{2+}$ from the ternary enzyme–$Mn^{2+}$–pdTp complexes, was determined for each mutant by titrations of equimolar solutions of enzyme and 3′,5′-pdTp with $Mn^{2+}$, monitoring $Mn^{2+}$ binding by EPR and by the effects of bound $Mn^{2+}$ on $1/T_1$ of water protons. Scatchard plots of both the EPR data (Fig. 5B) and $1/T_1$ data (not shown) yielded approximately one tight binding site for $Mn^{2+}$ with the $K_A'$ values listed in Table IV. For each mutant, the $n$ and $K_A'$ value obtained by both methods agreed within experimental error. Comparison of $K_A'$ with $K_D$ indicates that the presence of the inhibitor 3′,5′-pdTp increases the affinity of the wild-type enzyme and K49A, K84A, Y115A mutants for $Mn^{2+}$ by factors of 398, 627, 100, and 310, respectively.

The dissociation constants of the inhibitor 3′,5′-pdTp from the ternary enzyme–$Mn^{2+}$–3′,5′-pdTp complex were determined for each mutant by titrations of solutions of enzyme and $Mn^{2+}$ with 3′,5′-pdTp measuring changes in the enhancement ($\epsilon^*$) of $1/T_{1p}$ of water protons.[22] The titration curves were fit with the known values of $K_D$(Mn), $K_A'$ (Mn), and $K_1$ and with computed values of $K_S$, $K_2$ (Mn), and $K_3$ (Mn) (Fig. 7). The computed equilibrium constants (Table IV) indicate that, in the absence of metal, the K49A and Y115A mutations significantly weaken 3′,5′-pdTp binding to the enzyme as shown by 4.4 ± 1.8 and 3.6 ± 1.6-fold increases in $K_S$, respectively, while the K84A mutation had no effect on $K_S$ (1.5 ± 0.7-fold). The dissociation constant of $Mn^{2+}$–3′,5′-pdTp from the ternary enzyme–$Mn^{2+}$–3′,5′-pdTp complex, $K_2$, is 2.0 ± 0.8-fold greater with the Y115A mutant than with the wild-type enzyme, but unaltered with the K84A and K49A mutants (Table IV).†

### Ternary Enzyme–$Ca^{2+}$–3′,5′-pdTp Complexes

$K_A'$ (Ca), the dissociation constant of $Ca^{2+}$ from the ternary enzyme–$Ca^{2+}$–3′,5′-pdTp complex, was determined by $Ca^{2+}$ titration in competition with $Mn^{2+}$ monitoring both the decrease in the enhancement ($\epsilon^*$) of $1/T_{1p}$ of water protons (Fig. 6) and the appearance of free $Mn^{2+}$ by EPR. The resulting values of $K_A'$ (Ca) (Table V) indicate that the K84A mutation slightly weakens $Ca^{2+}$ binding in the ternary complex while the other mutations have no effect. The dissociation constant $K_2$ of $Ca^{2+}$–3′,5′-pdTp from the ternary enzyme–$Ca^{2+}$–3′,5′-pdTp complex, calculated from the measured values of $K_A'$ (Ca), $K_S$, and $K_1$ (Ca) with the relationship $K_2 = K_A' \cdot K_S/K_1$ (Tables IV, V), indicates decreased affinities of $Ca^{2+}$–3′,5′-pdTp for each mutant, as compared to the wild-type enzyme, by factors of 4.5 ± 1.6, 3.7 ± 1.4, and 4.7 ± 1.7 for the K49A, K84A, and Y115F mutants, respectively (Table V).†

## DISCUSSION

Comparisons of protein structures determined by both NMR and X-ray methods have shown that solution and crystal structures of a protein are generally in agreement.[28] Structural differences are minimal for residues in well-ordered secondary structural elements and in the interior of the protein. Residues at protein surfaces have the most pronounced differences which are commonly attributed to the effects of crystal packing. Such crystal pack-

†The mutant enzymes interact more weakly with divalent cations as revealed by increases in $K_D$ and $K_A'$. This permits the enzyme-bound metal ions to interact more strongly with the added ligand 3′,5′-pdTp, resulting in net decreases in the $K_3$ values (Tables IV, V).

**TABLE IV. Dissociation Constants (μM) and Enhancement Factors of Binary and Ternary Complexes of Staphylococcal Nuclease, $Mn^{2+}$, and 3′,5′-pdTp***

| Enzyme | $n$ | $K_D$[†] | $n$ | $K_A'$[‡] | $K_3$[§] | $K_S$[§] | $K_2$ | $\epsilon_b$ | $\epsilon_T$ |
|---|---|---|---|---|---|---|---|---|---|
| WT | 0.97 ± 0.04 | 438 ± 85 | 0.94 ± 0.06 | 1.10 ± 0.60 | 2.50 ± 1.00 | 94 ± 38 | 2.2 ± 0.9 | 8.4 ± 0.7 | 24.8 ± 0.4 |
| K49A | 1.00 ± 0.05 | 1774 ± 150 | 1.01 ± 0.10 | 2.83 ± 0.31 | 0.66 ± 0.06 | 409 ± 31 | 2.44 ± 0.18 | 15.0 ± 2.0 | 24.4 ± 0.4 |
| K84A | 1.14 ± 0.10 | 950 ± 172 | 1.20 ± 0.10 | 9.54 ± 2.06 | 1.42 ± 0.35 | 141 ± 35 | 2.84 ± 0.71 | 11.6 ± 1.4 | 22.6 ± 0.4 |
| Y115A | 1.18 ± 0.10 | 1948 ± 241 | 1.15 ± 0.10 | 6.28 ± 0.70 | 1.08 ± 0.13 | 335 ± 76 | 4.44 ± 0.53 | 15.0 ± 3.0 | 27.7 ± 0.5 |

*The dissociation constants of the ternary and relevant binary complexes of enzyme (E), metal (M), and ligand (L) are defined as follows:[31] $K_1$ = [M][L]/[M–L]; $K_D$ = [E][M]/[E–M]; $K_2$ = [E][M–L]/[E–M–L]; $K_A'$ = [E–L][M]/[E–M–L]; $K_3$ = [E–M][L]/[E–M–L]; $K_S$ = [E][L]/[E–L]. Relationship: $K_1K_2 = K_3K_D = K_A'K_S$. The parameters for the wild-type enzyme and $K_1$ (474 ± 50 μM) are from Serpersu et al.[12]

[†]Determined by EPR, as in Figure 5A.

[‡]Determined by EPR, as in Figure 5B.

[§]Determined by computer analysis of pdTp titration as in Figure 7.[22]

**TABLE V. Dissociation Constants (μM) of Ternary Enzyme–$Ca^{2+}$–3′,5′-pdTp Complexes of Wild-Type and Mutant Staphylococcal Nuclease***

| Enzyme | $K_D$[†] | $K_S$[‡] | $K_A'$[†] | $K_2$[§] | $K_3$[**] | $K_1$ |
|---|---|---|---|---|---|---|
| WT | 510 ± 70 | 94 ± 38 | 71 ± 8 | 5.6 ± 1.9 | 13.1 ± 5.8 | 1200 ± 700 |
| K49A | 4642 ± 560 | 409 ± 31 | 74 ± 10 | 25.2 ± 2.2 | 6.6 ± 0.9 | 1200 ± 700 |
| K84A | 4849 ± 1250 | 141 ± 35 | 175 ± 44 | 20.6 ± 3.9 | 5.1 ± 1.6 | 1200 ± 700 |
| Y115A | 5044 ± 950 | 335 ± 76 | 94 ± 17 | 26.2 ± 3.7 | 6.2 ± 1.4 | 1200 ± 700 |

*The dissociation constants of the ternary and relevant binary complexes of enzyme, metal, and ligand are defined in Table IV. All parameters for WT and $K_1$ (1200 ± 700 μM) are from Serpersu et al.[12]

[†]Determined by competition with $Mn^{2+}$ measuring $1/T_1$ of water protons (Fig. 6).

[‡]From Table IV.

[§]Based on $K_A'K_S/K_1$.

[**]Based on $K_A'K_S/K_D$.

ing effects may induce structural changes in localized regions of a protein especially in long, flexible side chains (e.g., Lys) from an adjacent molecule in the crystal lattice.

A comparison of the X-ray structure of the staphylococcal nuclease–$Ca^{2+}$–3′,5′-pdTp complex[2] with the NMR docked structure determined in solution[6] reveals that in the crystal, the conformation of 3′,5′-pdTp is distorted by Lys-70* and Lys-71* from an adjacent molecule of the enzyme, resulting in a sizable rotation of 115 ± 31° about the C4′–C5′ bond and a rotation of at least 26° about the C5′–O5′ bond of the bound nucleotide (Fig. 1). While the 5′-phosphate of 3′,5′-pdTp in the NMR docked structure overlaps with that in the X-ray structure, the thymine, deoxyribose, and 3′-phosphate are displaced from their positions in the X-ray structure, resulting in differences in hydrogen bonding in the two structures. Thus, in the NMR-docked structure the 3′-phosphate of pdTp accepts a hydrogen bond from the ϵ-amino group of Lys-49 (2.89 Å) rather than from that of Lys-84 (8.63 Å) or Tyr-85 (4.85 Å), and the $N_3H$ of thymine donates a hydrogen bond to the OH of Tyr-115 (3.16 Å) which does not occur in the X-ray structure (5.28 Å) (Fig. 1, Table I).

As an independent test of these interactions, the binding of 3′,5′-pdTp to the K49A, K84A, and Y115A mutants was studied. Each mutant was fully active, and structurally intact as found by CD and by 2D $^1H$ NMR spectroscopy. In the binary enzyme–3′,5′-pdTp complex, the K84A mutant shows a negligible 1.5 ± 0.7-fold increase in $K_S$, the K49A mutant shows a 4.4 ± 1.8-fold increase, and the Y115A mutant shows a 3.6 ± 1.6-fold increase in $K_S$ (Table V). Although these effects are small, they are consistent with the loss of hydrogen bonds found in the NMR-docked structure of the enzyme–$Ca^{2+}$–3′,5′-pdTp ternary complex and are not readily explained by the X-ray structure (Fig. 1). Similar 4- to 5-fold weakening of binding of $Ca^{2+}$–3′,5′-pdTp is found in the ternary complexes of each of the three mutants K49A, K84A, and Y115A, as reflected in increased $K_2$ values (Table V). These results are not explained by the X-ray structure, but are consistent with the NMR docked structure, provided that the 3.53 Å distance from Nϵ of Lys-84 to N3 of the thymine ring of 3′,5′-pdTp represents a weak hydrogen bond (Table I). While unlikely, it cannot be excluded that the weakened binding of 3′,5′-pdTp and its $Ca^{2+}$ complex to the K49A and Y115A mutants, but not to the K84A mutant, might result from structural alterations which are too small to be detected by NMR and CD.

The major thermodynamic effect at the active site of the K49A, K84A, and Y115A mutations was on the binding of divalent cations. Thus, the three mutants described here, and the R35G and R87G mutations previously studied[13] weaken the binding of

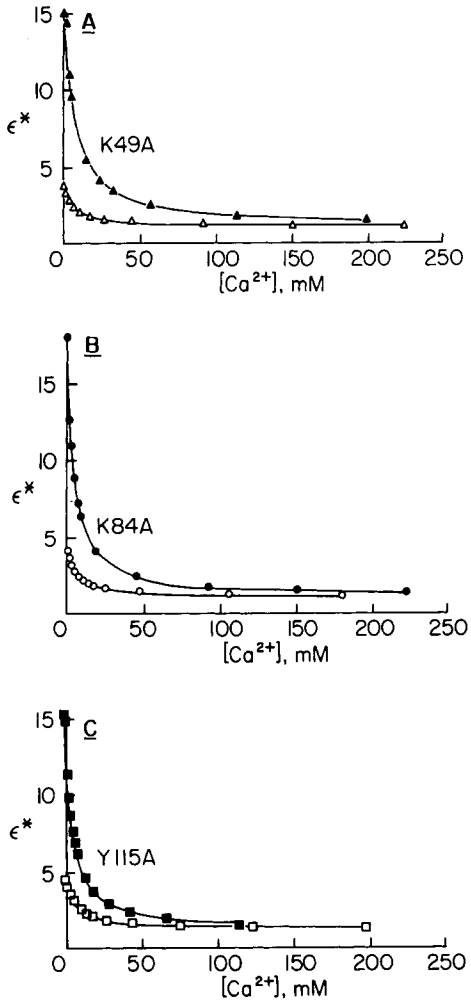


Fig. 6. Displacement of $Mn^{2+}$ by $Ca^{2+}$ from various binary and ternary complexes of staphylococcal nuclease monitored by changes in the enhancement ($\epsilon^*$) of the effects of $Mn^{2+}$ on $1/T_1$ of water protons. (**A**) Displacement of $Mn^{2+}$ by $Ca^{2+}$ from complexes of K49A. The solution contained either 483 μM K49A with 163 μM $MnCl_2$ (△) or 483 μM K84A with 305 μM $MnCl_2$ and 491 μM 3′,5′-pdTp (▲). (**B**) Displacement of $Mn^{2+}$ by $Ca^{2+}$ from complexes of K84A. The solution contained either 516 μM K84A with 281 μM $MnCl_2$ (○) or 521 μM K84A with 160 μM $MnCl_2$ and 487 μM 3′,5′-pdTp (●). (**C**) Displacement of $Mn^{2+}$ by $Ca^{2+}$ from complexes of Y115A. The solution contained either 712 μM K84A with 168 μM $MnCl_2$ (□) or 475 μM K84A with 288 μM $MnCl_2$ and 487 μM 3′,5′-pdTp (■). Titration curves were computed using the $K_D$ and $K_A'$ values given in Tables IV and V. Other components are as given in Figure 5.

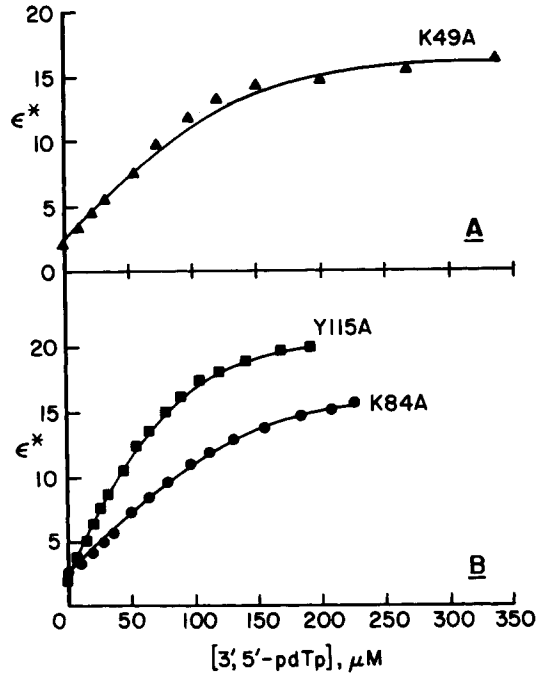


Fig. 7. Titrations of $Mn^{2+}$ complexes of K49A, K84A, and Y115A mutants with 3′,5′-pdTp, measuring the changes in enhancement ($\epsilon^*$) of the paramagnetic effects of $Mn^{2+}$ on the $1/T_1$ of water protons. (**A**) Titration of the K49A with 3′,5′-pdTp. The solution contained 163.7 μM K49A with 201 μM $MnCl_2$ (▲). (**B**) Titration of the K84A (●) and Y115A mutants with 3′,5′-pdTp (■). The solutions contained either 169 μM K84A with 170 μM $MnCl_2$ or 161 μM K84A with 162 μM $MnCl_2$. Other components are as given in Figure 5.

$Mn^{2+}$ and $Ca^{2+}$ to staphylococcal nuclease and to its 3′,5′-pdTp complex by an order of magnitude (Tables II, IV, and V) even though these mutations do not involve direct ligands of the metal. Changes in the liganding environment of enzyme-bound $Mn^{2+}$ in the mutants are also indicated by altered enhancement factors for the binary ($\epsilon_b$) and ternary complexes ($\epsilon_T$) (Table IV). These indirect effects of mutations on metal binding and environment which are comparable in magnitude to the effects of loss of a direct ligand[12] indicate that staphylococcal nuclease is susceptible to conformational changes at the metal binding site. By the systematic replacement of hydrophobic residues throughout staphylococcal nuclease, Shortle et al.[29] found that mutations in one region of the enzyme, the 5-stranded β-barrel, increased the sensitivity of the enzyme to denaturation with GuHCl while such mutations in the carboxy-terminal third of the enzyme decreased the sensitivity to GuHCl, suggesting that the enzyme consists of two subdomains. Preliminary X-ray scattering studies of the denatured state revealed a bilobed structure, supporting the existence of two subdomains which have a tendency to separate.[29] Wang et al.,[27] by comparing X-ray and NMR structures of free and ligated staphylococcal nuclease, have noted conformation changes in both of these regions of the enzyme upon binding of $Ca^{2+}$ and 3′,5′-pdTp. Interestingly, one of the two strong ligands of $Ca^{2+}$, Asp-21 is on one of these subdomains, the 5-stranded β-barrel, and the other strong ligand, Asp-40, is linked to the carboxy-terminal subdomain. While denaturation, of course, represents an extreme conformational change, smaller conformational changes induced by mutations could separate these subdomains, pulling apart the $Ca^{2+}$ ligands, thus weakening metal binding. Consistent

with such an effect, the enlargement of Asp-21 to Glu partially restores tight metal binding and increases the catalytic activity of the R87G mutant.[30]

## CONCLUSIONS

Differences between the hydrogen bonding of 3′,5′-pdTp found in the X-ray structure and in the NMR-docked structure of the staphylococcal nuclease-metal-3′,5′-pdTp complex were tested by studies of the K49A, K84A and Y115A mutants. While structurally intact as revealed by catalytic activity, CD spectroscopy, and 2D NMR studies, the three mutant enzymes bound divalent cations more weakly, and showed altered relaxation effects of $Mn^{2+}$ indicating a change in the environment of the metal. These effects may result from an inherent tendency of staphylococcal nuclease to open into two subdomains, separating the two strong ligands of $Ca^{2+}$, Asp-21 and Asp-40. In the binary enzyme–3′,5′-pdTp complex, the K49A and Y115A mutant enzymes showed weaker binding of 3′,5′-pdTp, and in the ternary enzyme–$Ca^{2+}$-3′,5′-pdTp complexes, all three mutants showed weaker binding of $Ca^{2+}$–3′,5′-pdTp. Although the thermodynamic effects of these mutations on the binding of 3′,5′-pdTp and its $Ca^{2+}$ complex are small, corresponding to the loss of 0.8 ± 0.2 kcal/mol in binding free energy, they can be explained by the NMR-docked structure but not by the X-ray structure.

## ACKNOWLEDGMENTS

We are grateful to Alan Meeker and David Shortle for providing the clones of the mutant enzymes, to C. Abeygunawardana for help with the NMR instrumentation, to G. D. Fasman for providing his program for the analysis of CD spectra, and to Peggy Ford for secretarial assistance. Supported by National Institutes of Health Grant (DK-28616) to A.S.M. D.J.W. is a recipient of a National Institutes of Health National Research Service Award (F32 GM13324).

## REFERENCES

1. Cotton, F. A., Hazen, E. E., Jr., Legg, M. J. Staphylococcal nuclease: Proposed mechanism of action based on structure of enzyme-thymidine 3′,5′-bisphosphate-calcium ion complex at 1.5 Å resolution. Proc. Natl. Acad. Sci. U.S.A. 76:2551–2555, 1979.
2. Loll, P. J., Lattman, E. E. The crystal structure of the ternary complex of staphylococcal nuclease, $Ca^{2+}$, and inhibitor pdTp, refined at 1.65 Å. Proteins 5:183–201, 1989.
3. Torchia, D. A., Sparks, S. W., Bax, A. Staphylococcal nuclease: Sequential assignments and solution structure. Biochemistry 28:5509–5524, 1989.
4. Wang, J., LeMaster, D. M., Markley, J. L. Two-dimensional NMR studies of staphylococcal nuclease. I. Sequential specific assignments of hydrogen-1 signals and solution structure of the nuclease H124L-3′,5′-pdTp-$Ca^{2+}$ ternary complex. Biochemistry 29:88–101, 1990.
5. Baldisseri, D. M., Torchia, D. A., Poole, L. B., Gerlt, J. A. Deletion of the Ω-loop in the active site of staphylococcal nuclease. 2. Effects on protein structure and dynamics. Biochemistry 30:3628–3633, 1991.
6. Weber, D. J., Serpersu, E. H., Gittis, A. G., Lattman, E. E., Mildvan, A. S. NMR docking of the competitive inhibitor thymidine 3′,5′-diphosphate into the X-ray structure of staphylococcal nuclease. Proteins 17:20–35, 1993.
7. Serpersu, E. H., Hibler, D. W., Gerlt, J. A., Mildvan, A. S. Kinetic and magnetic resonance studies of the glutamate-43 to serine mutant of staphylococcal nuclease. Biochemistry 28:1539–1548, 1989.
8. Grissom, C. B., Markley, J. L. Staphylococcal nuclease active site amino acids: pH dependence of tyrosines and arginines by $^{13}C$ NMR and correlation with kinetic studies. Biochemistry 28:2116–2124, 1989.
9. Cuatrecasas, P., Fuchs, S., Anfinsen, C. B. Catalytic properties and specificity of the extracellular nuclease of staphylococcus aureus. J. Biol. Chem. 242:1541–1547, 1967.
10. Shortle, D., Lin, B. Genetic analysis of staphylococcal nuclease: Identification of three intragenic "global" suppressors of nuclease-minus mutations. Genetics 110:539–555, 1985.
11. Shortle, D., Meeker, A. K. Residual structure in large fragments of staphylococcal nuclease: Effects of amino acid substitutions. Biochemistry 28:936–944, 1989.
12. Serpersu, E. H., Shortle, D. R., Mildvan, A. S. Kinetic and magnetic resonance studies of the effects of genetic substitution of a $Ca^{2+}$-liganding amino acid in staphylococcal nuclease. Biochemistry 25:68–77, 1986.
13. Serpersu, E. H., Shortle, D. R., Mildvan, A. S. Kinetic and magnetic resonance studies of active site mutants of staphylococcal nuclease: Factors contributing to catalysis. Biochemistry 26:1289–1300, 1987.
14. Cleland, W. W. Statistical analysis of enzyme kinetic data. Methods Enzymol. 63A:103–138, 1979.
15. Chen, G. C., Yang, J. T. Two-point calibration of circular dichrometer with d-10-camphorsulfonic acid. Anal. Lett. 10(14):1195–1207, 1977.
16. Perczel, A., Hollosi, M., Tusnady, G., Fasman, G. Convex constraint analysis: A natural deconvolution of circular dichroism curves of proteins. Protein Eng. 4:669–679, 1991.
17. Perczel, A., Park, K., Fasman, G. D. Analysis of the circular dichroism spectrum of proteins using the convex constraint algorithm: A practical guide. Anal. Biochem. 203: 83–93, 1992.
18. Yang, Y. T., Wu, C.-S. C., Martinez, H. M. Calculation of protein conformation from circular dichroism. Methods Enzymol. 130:208–269, 1986.
19. Jeener, J., Meier, B. H., Bachmann, P., Ernst, R. R. Investigation of exchange processes by two-dimensional NMR spectroscopy. J. Chem. Physics 71:4546–4553, 1979.
20. Marion, D., Wüthrich, K. Applications of phase sensitive two dimensional correlated spectroscopy (COSY) for measurements of $^1H$-$^1H$ spin-spin coupling constants in proteins. Biochem. Biophys. Res. Commun. 113:967–974, 1983.
21. Carr, H. Y., Purcell, E. M. Effects of diffusion on free precession in nuclear magnetic resonance experiments. Phys. Rev. 94:630–638, 1954.
22. Mildvan, A. S., Engle, J. L. Nuclear relaxation measurements of water protons and other ligands. Methods Enzymol. 49G:322–359, 1972.
23. Cohn, M., Townsend, J. A study of manganous complexes by paramagnetic resonance spectroscopy. Nature (London) 173:1090–1091, 1954.
24. Mildvan, A. S., Cohn, M. Magnetic resonance studies of the interaction of the manganous ion with bovine serum albumin. Biochemistry 2:910–919, 1963.
25. Reed, G. H., Cohn, M., O'Sullivan, W. J. Analysis of equilibrium data from proton magnetic relaxation rates of water for manganese-nucleotide-kinase ternary complexes. J. Biol. Chem. 245:6547–6552, 1970.
26. Hynes, T. R., Fox, R. O. The crystal structure of staphylococcal nuclease refined at 1.7 Å resolution. Proteins 10:92–105, 1991.
27. Wang, J., Linck, A., Loh, S. N., LeMaster, D. M., Markley, J. L. Solution studies of staphylococcal nuclease H124L. 2. $^1H$, $^{13}C$, and $^{15}N$ chemical shift assignments for the unligated enzyme and analysis of chemical shift changes that accompany formation of the nuclease-thymidine 3′,5′-bisphosphate-calcium ternary complex. Biochemistry 31: 921–930, 1992.
28. Baldwin, E. T., Weber, I. T., Charles, R. S., Xuan, J.-C.,

Appella, E., Yamada, E., Matsushima, K., Edwards, B. F. P., Clore, G. M., Gronenborn, A. M., Wlodawer, A. Crystal structure of interleukin 8: Symbiosis of NMR and crystallography. Proc. Natl. Acad. Sci. U.S.A. 88:502–510, 1991.
29. Shortle, D., Stites, W. E., Meeker, A. K. Contributions of the large hydrophobic amino acids to the stability of staphylococcal nuclease. Biochemistry 29:8033–8041, 1990.
30. Weber, D. J., Serpersu, E. H., Shortle, D., Mildvan, A. S. Diverse interactions between the individual mutations in a double mutant at the active site of staphylococcal nuclease. Biochemistry 29:8632–8642, 1990.
31. Mildvan, A. S., Cohn, M. Kinetic and magnetic resonance studies of the pyruvate kinase reaction. II. Complexes of enzyme, metal, and substrates. J. Biol. Chem. 241:1178–1193, 1966.